Personalized Bioconversion of Panax Notoginseng Saponins Mediated by Gut Microbiota Between Chinese-diet and Western-diet Healthy Subjects

Li Wang
Xiangya Hospital Central South University
Man-Yun Chen
Xiangya Hospital Central South University
Li Shao
Hunan University of Chinese Medicine
Wei Zhang
Xiangya Hospital Central South University
Xiang-Ping Li
Xiangya Hospital Central South University
Wei-Hua Huang (endeavor34852@aliyun.com)
Xiangya Hospital Central South University https://orcid.org/0000-0003-4167-8304

Research

Keywords: Panax notoginseng saponins, Gut microbiota, 16S rRNA gene sequencing, Metabolic difference, Biotransformation

Posted Date: May 11th, 2021

DOI: https://doi.org/10.21203/rs.3.rs-500625/v1

Version of Record: A version of this preprint was published at Chinese Medicine on July 23rd, 2021. See the published version at https://doi.org/10.1186/s13020-021-00476-5.

Abstract

Background: *Panax notoginseng* saponins (PNS) as the main effective substances from *P. notoginseng* with low bioavailability could be bio-converted by human gut microbiota. In our previous study, PNS metabolic variations mediated by gut microbiota have been observed between high fat, high protein (HF-HP)-diet and low fat, plant fiber-rich (LF-PF)-diet subjects. In this study, we aimed to correspondingly characterize the relationship between distinct gut microbiota profiles and PNS metabolites.

Methods: Gut microbiota were collected from HF-HP and LF-PF healthy adults, respectively and profiled by 16S rRNA gene sequencing. PNS were incubated with gut microbiota in vitro. A LC-MS/MS method was developed to quantify the five main metabolites yields including ginsenoside F_1 (GF_1), ginsenoside Rh_2 (GRh_2), ginsenoside compound K (GC-K), protopanaxatriol (PPT) and protopanaxadiol (PPD). The selected microbial species, *Bifidobacterium adolescentis* and *Lactobacillus rhamnosus*, were employed to metabolize PNS for the corresponding metabolites.

Results: The five main metabolites were significantly different between the two diet groups. Compared with HF-HP group, the microbial genus *Blautia*, *Bifidobacterium, Clostridium, Corynebacterium, Dorea, Enhydrobacter*, *Lactobacillus, Roseburia*, *Ruminococcus, SMB53, Streptococcus, Treponema* and *Weissella* were enriched in LF-PF group, while *Phascolarctobacterium* and *Oscillospira* were relatively decreased. Furthermore, Spearman's correlative analysis revealed gut microbiota enriched in LF-PF and HF-HP groups were positively and negatively associated with PNS metabolites yields, respectively.

Conclusions: Our data showed gut microbiota diversity led to the personalized bioconversion of PNS.

Introduction

Panax notoginseng saponins (PNS) as the main health-beneficial components in *P. notoginseng* are limited with low bioavailability due to their poor membrane permeability[1]. However, after orally administrated, PNS inevitably interact with gut microbiota in gastrointestinal tract, which could be bio-converted to be novel bioactive metabolites[2, 3]. For PNS metabolism, gut microbiota are mainly involved in deglycosylation reaction with hydrolyzing the oligosaccharide chains, which are catalyzed by the microbial *β*-glycosidases[4, 5]. Recently, some reports have focused on the PNS bioconversion mediated by gut microbiota to reveal the metabolic profile of PNS[4, 6]. However, in our previous study, significant variations of PNS metabolism were discovered between two different dietary-induced human gut microbiota groups[7]. Undoubtedly, the metabolic variations will alter the pharmacological effects of PNS. Due to the complex gut microbiome community characterized with different xenobiotic-metabolizing enzymes, the accurate metabolism profile of PNS still remains largely elusive.

Beside the intrinsic host genetic makeup, gut microbiota possess a dynamic balance with external environment exposure, such as nutritional state and disease status. The most effective determining factor is the daily dietary pattern of healthy subjects, which could modulate the profile of gut microbiota[8]. Obviously, the personalized microbial phylotypes will lead to the metabolic variations of PNS. Therefore, the inter-diversity of gut microbiota between HF-HP and LF-PF groups was the focal point in this study, instead of focusing on the intra-group differences.

The key development of high-throughput sequencing technology as a perspective application make it possible to insight into the composition, diversity, even the gene functions of gut microbial communities through the analysis of 16S rRNA sequencing or whole-genome shotgun sequencing[9, 10]. Herein, to clarify the metabolism differences of PNS pertinent to gut microbiota, it was necessary to elucidate the relationship between PNS metabolites and bacterial communities driven by different diet patterns.

In the present study, the different gut microbiota were randomly collected from six western-diet (HF-HP) and six Chinese-diet (LF-PF) healthy subjects, respectively. The V3-V4 region of 16S rRNA gene was sequenced on an Illumina HiSeq 2500. The main metabolites of PNS (GF_1, GRh_2, GCK, PPT and PPD) were relatively quantified by a high performance liquid chromatography-electrospray ionization tandem mass spectrometry (HPLC-ESI-MS/MS). Alpha- and beta-diversities were employed to evaluate the richness and evenness of gut microbiota complexity. Both of Operational Taxonomic Units(OTUs) and predictive functional profiles of gut microbial communities were used to estimate the inter-difference between the two groups. Moreover, *Bifidobacterium adolescentis* and *Lactobacillus rhamnosus* were selected as a representative species of *Bifidobacterium* and *Lactobacillus* to verify the results. Altogether, our data indicated that the composition and diversity of gut microbial communities could be modulated by diet composition, which could lead to metabolic variations of PNS.

Materials And Methods

Chemicals and reagents

General anaerobic medium (GAM) broth was obtained from Nissui Pharmaceutical Inc. (Tokyo, Japan). Leibovitz's L-15 medium was purchased from Life Technologies Co. (Grand Island, NY, USA). Brain heart infusion (BHI) broth was manufactured from Oxoid Ltd. (Basingstoke, England). Fetal bovine serum (FBS) was purchased from Gibco (Gaithersburg, MD, USA). HPLC-grade acetonitrile (ACN) was purchased from Merck (Darmstadt, Germany). Deionized water (18 MΩ cm^{-1}) was purified using a Milli-Q Ultrapure water system (Milford, MA, USA). Ginsenoside F1, GRh2, and PTT were bought from Baoji Herbest Bio-Tech Co., Ltd. (Shaanxi, China). GC-K, PPD and digoxin (the internal standard, IS) were provided

by Chengdu Push Bio-technology Co., Ltd. (Sichuan, China). The purity of all compounds was determined by HPLC (≥ 98%), and their chemical structures were shown in Fig. 1.

Bacteria genomic DNA extraction kit was purchased from Omega Bio-tek (Norcross, GA, USA). Mixture Polymerase Chain Reaction (PCR) product purification kit was purchased from Qiagen (Hilden, Germany). Sequencing library generation kit was purchased from Illumina (San Diego, USA).

Sample collection and gut microbiota preparation

Stool samples were collected from Chinese-diet and western-diet pattern healthy subjects. Inclusion criteria were following as, (i) age between 20 and 25 years; (ii) body mass index (BMI) between 19-24 kg/m^2; (iii) absence of systemic and metabolic disease; (iv) no use of alcohol and tobacco; and (v) stable diet patterns in the last one year, pertinent to HF-HP and LF-PF diets. Exclusion criteria were defined as, (i) history of any antibiotics or probiotics medications in the last three months; (ii) history of drug allergies and highly sensitive to environmental; and (iii) mental illness rendering the participants unable to understand the nature, scope, and possible consequences of the study. All individuals provided written informed consent prior to participating in the study.

According to our previous study[7], 1 g of fresh fecal sample was suspended in 20 mL of cold physiological saline and then centrifuged to collect the resultant fecal supernatant. The precipitation was re-suspended with Leibovitz's L-15 medium containing glycerol as the gut microbiota solution stored in −80 ℃ freeze.

PNS preparation and incubation

The air-dried root of *P. notoginseng* was purchased from Wenshan city (Yunnan, China) and extracted by heat-refluxing with 70% ethanol to obtain the *P. notoginseng* extract. The detailed information about *P. notoginseng* and PNS extraction were described in our former publication[7].

Gut microbiota stock was activated with GAM broth and then centrifuged to collect the gut microbiota precipitation. Leibovitz's L-15 medium was added to re-suspend the precipitate as the gut microbiota work solution. Gut microbiota work solution, *P. notoginseng* extract stock solution in dimethyl sulphoxide (DMSO) and Leibovitz's L-15 medium were mixed as incubation system incubated at 37 ℃ for 48 h. The reaction mixtures were successively extracted by ethyl acetate and n-butanol, and evaporated under nitrogen. At last, the samples were reconstituted with methanol before subjected to HPLC analysis. The specific plan was described in our previous study[7].

Bifidobacterium adolescentis and *Lactobacillus rhamnosus* were cultured in Reinforced Clostridium Medium （RCM）and Brain Heart Infusion Medium （BHI）broth containing 10% FBS for 24 h before incubation 48 h with PNS at 37 ℃. The reaction mixtures were extracted as the same with above-mentioned methods.

Relative quantification of metabolites by HPLC- MS

The PNS metabolites biotransformed by intestinal microbiota were quantified by comparing the five main metabolites between LF-PF and HF-HP diet group on an HPLC-ESI-MS/MS system, which consisted of a SHIMADZU Nexera X2 HPLC system (SHIMADZU, Tokyo, Japan) and AB SCIEX Triple Quad TM 6500 mass spectrometers equipped with electrospray ionization (AB SCIEX, CA, USA). Take our previous method and adjust it accordingly[11], the chromatographic separation was performed on an Phenomenex LUNA C18 (2) Reversed Phase (150 mm × 2.0 mm, 5 μm) with a gradient elution of 0.1% formic acid in water (A) and ACN (B) at a flow rate of 0.3 mL/min. The gradient profile was optimized below, 0–2 min: 35%–65% B, 2–6 min: 65%–70% B, 6–7 min: 70%–72% B, 7–7.5 min: 72%–85% B, 7.5–8 min: 85%–85% B, 8–11 min: 85%–95% B,11–12 min: 95%–100% B. The injection volume was 2 μL and the temperature of column was set at 40 ℃. The following mass spectrometer parameters were selected in positive ion mode,spray voltage:4500 V; temperature:350 ℃; collision gas: 10 psi; curtain gas: 35 psi; ion source gas 1: 55 psi; ion source gas 2: 50 psi.

Method validation

Five metabolites including GF1, Rh2, GC-K, PPD, PPT and digoxin (IS) were mixed and dissolved in methanol to validate this method. For intra-day precision, the dissolved standards were analyzed three times within one day, while they were determined in triplicate for three continuous days for inter-day precision. Relative standard deviations (RSDs) were calculated to assess the variations. Selectivity was investigated by comparing the spectra of blank human gut microbiota with IS or with analytes and IS to exclude the peaks of endogenous components in incubating system.

DNA extraction and PCR amplification

Microbial genomic DNA was extracted from each sample and stored in -20 ℃ using the Qiagen QIAamp DNA Stool Mini Kit (Qiagen). DNA concentration and molecular weight were estimated using a nanodrop instrument (Thermo Scientific), and the purity of DNA were monitored on 1% agarose gels. Subsequently, DNA was diluted to 1 ng/μL using sterile water. The variable region V3-V4 of the bacteria 16S rRNA gene from each sample were amplified using the bacterial universal primer 338F 5'- ACTCCTACGGGAGGCAGCAG-3' and 806R 5'-barcode GGACTACHVGGGTWTCTAAT-3', while barcode is a six-base unique sequence to each sample. All PCR reactions were carried out in 20 μL of

reactions with 4 μL of 5 × FastPfu Buffer, 2 μL of 2.5 mM dNTPs, 0.8 μL of each primer (5 μM), 0.4 μL of FastPfu Polymerase, and 10 ng of template DNA. PCR thermal cycling conditions were initial denaturation at 98 ℃ for 1 min, followed by 30 cycles of denaturation at 98 ℃ for 10 s, annealing at 50 ℃ for 30 s and elongation at 72 ℃ for 30 s, with a final extension at 72 ℃ for 5 min.

MiSeq sequencing of 16S rRNA gene amplicons

The PCR products of the same sample were mixed firstly, and then extracted from 2% agarose gels and purified using the AxyPrep DNA Gel Extraction Kit (Axygen Biosciences, Union City, CA, U.S.) according to the manufacturer's instructions. Referring to the preliminary quantitative results of electrophoresis, QuantiFluor™ -ST blue fluorescence quantitative system was used to detect and quantify the PCR products. Purified amplicons were pooled in equimolar and paired-end sequenced (2 × 250) on an Illumina MiSeq platform according to the standard protocols.

Bioinformatics analysis

Paired-end reads were assigned to samples based on their unique barcode and truncated by cutting off the barcode and primer sequence, and then merged using FLASH (V1.2.7, http://ccb.jhu.edu/software/FLASH/). Quality filtering on the raw tags were performed to obtain the clean tags according to the QIIME2 software (Version 2018.11 https://qiime2.org) quality control process. The Dada2 plugin was used for quality filtering , and then the Vsearch plugin was used to remove the chimera of the data to obtain Clean Data. Sequences analysis was performed using Vsearch plugin, and sequence with ≥ 97% similarity was assigned to the same OTUs. Representative sequence for each OTU was screened and annotated for taxonomic information based on the GreenGene Database (http://greengenes.lbl.gov/cgi-bin/nph-index.cgi). QIIME2 software package in-house Perl scripts were used to analyze alpha- (within samples) and beta- (among samples) diversity with normalized data to evaluate differences of samples in species richness and complexity.

In order to analyze alpha-diversity, Shannon index, Faith's index and Pielou's index were used to indicate the richness and diversity of the community, phylogenetic diversity and evenness, respectively. Observed OTUs were used to indicate abundance. The results were visualized using R software (Version 2.15.3). In order to analyze beta- diversity Bray-Curtis distance and Jaccard distance were calculated according to phylogenetic measures, while Unweighted Unifrac distance and Weighted Unifrac distance were employed for the sequence measures

A heat map was constructed with a cluster tree using the Microeco bioinformatics cloud (https://www.bioincloud.tech). LEfSe analysis was performed using LEfSe software to assess the effective size (LED> 2) of each differentially abundant taxon, while the cladogram was displayed according to effective size.

Statistical analysis

Spearman's correlation analysis and Student's *t*-test were performed using SPSS software (Version 23). Significant differences were set as * $p < 0.05$ and ** $p < 0.01$ or $q < 0.01$.

Results

Method validation

The intra-day variations (RSDs, n=12) of GF_1, GRh_2, PPD, PPT and GC-K were 8.77%,6.67%,8.37%,8.63% and 6.42%, respectively, and the inter-day RSDs were 13.4%,13.3%,13.3%,12.9% and 12.1%, respectively. The data indicated that the employed method was accurate and precise. This method displayed a good selectivity for the detection of all analytes. There was no significant endogenous interference around the chromatographic regions of analytes and IS in all blank human gut microbiota samples. Also, baseline separation has been achieved between IS and analytes (Fig. S1).

Biotransformation of PNS mediated by gut microbiota

In our previous study[7], forty-five metabolites of PNS were identified by HPLC-DAD-Q-TOF-MS/MS after incubating PNS with human gut microbiota *in vitro*. To evaluate the metabolic variations between HF-HP and LF-PF groups, five main metabolites were relatively quantified and compared with each other from different healthy subjects (Fig. 2A-E). The results showed the significant differences in the relative abundance of GRh_2, PPT and PPD between the two groups by *t*-test analysis ($p < 0.05$). Compared with HF-HP group, GRh_2, PPT and PPD were much higher in LF-PF group, but GF_1 and GC-K were much lower. Furthermore, the abundances of PPD-type secondary ginsenosides were significantly higher than PPT-type secondary ginsenosides in LF-PF group, who had stronger ability to metabolize PPD-type ginsenosides (Fig. 2F). Moreover, due to great individual variation, the considerable variation of metabolite amounts also occurred even within the same group.

Alpha- and beta-diversity of gut microbiota

As shown in the rarefaction curves (Fig. S2), the sequence reads were enough to perform species richness and evenness estimates. Compared with LF-PF group, the data showed a high bacterial diversity of gut microbiota in HF-HP group with higher richness (Fig. 3A). No significant alpha-

diversity metrics was found between the two diet groups. Other richness estimators, such as Observed OTUs and Faith's index, also revealed no statistically significant differences at OTU level (97%) (Fig. 3B and 3C). Evenness index (Fig. 3D) showed no discrimination between the two groups, indicating that the evenness of species was comparable between the two groups. Beta-diversity was evaluated by principal component analysis (PCoA). As shown in Fig. 3E-F, despite large inherent individual differences in gut microbiota appeared even within the same diet group, the results unambiguously supported that the PCoA plots could be divided into two clusters. The 16S rRNA sequencing data provided that the alpha- and beta-diversity of gut microbiota were significantly different between LF-PF group and HF-HP group.

Taxonomic differences of gut microbiota

We obtained an average of 1 374 features per DNA sample extracted from fecal samples of our cohort. Taxonomy-based comparisons of gut microbiota were performed to elucidate the overall community structure of gut microbiota on phyla and genus levels between the two groups. Relative abundance of the top ten gut microbials at phyla were shown in Fig. 4A and 4B, respectively. Compared with LF-PF group, the phyla Bacteroidetes, Cyanobacteria, Lentisphaerae, Proteobacteria, Spirochaetes, Verrucomicrobia and Tenericutes were enriched in HF-HP group, while Actinobacteria, Firmicutes and Fusobacteria decreased relatively. At the genus level, the top fifteen gut microbials were shown in Fig. 4C. Compared with HF-HP group, the genus *Blautia*, *Bifidobacterium*, *Roseburia*, *Ruminococcus* and *SMB53* were enriched in LF-PF group, while *Oscillospira* decreased relatively. A Clustering analysis based on the abundance of the top 25 features were transformed into a heat map, which revealed two main clusters (Fig. 4D). The results displayed the diversities of gut microbiota could be modulated by diet patterns.

We also used the linear discriminative analysis (LDA) effect size (LEfSe) biomarker discovery tool to identify taxonomic differences referring to diet patterns (Fig. 5A and 5B). In genus level, the biomarkers for the HF-HP cluster were *Oscillospira* and *Phascolarctobacterium*, while the biomarkers of LF-PF cluster were *Bifidobacterium*, *Blautia*, *Clostridium*, *Corynebacterium*, *Dorea*, *Enhydrobacter*, *Lactobacillus*, *Roseburia*, *Ruminococcus, SMB53, Streptococcus, Treponema* and *Weissella*. Moreover, *Blautia*, *Bifidobacterium*, *Roseburia*, *Ruminococcus, SMB53* and *Oscillospira* (Fig. 5C-H) were taxonomic differences with higher abundance in the genus level. These biomarkers presented high LDA scores (LDA > 2) and were enriched in Firmicutes and Actinobacteria phylum (Table1).

Table.1 Taxonomic differences of gut microbiota between LF-PF and HF-HP diet groups

No./Taxonomy	Kingdom	Phylum	Class	Order	Family	Genus
1	*Bacteria*	Firmicutes	Clostridia	Clostridiales	Lachnospiraceae	*Blautia*
2	*Bacteria*	Firmicutes	Clostridia	Clostridiales	Lachnospiraceae	*Roseburia*
3	*Bacteria*	Firmicutes	Clostridia	Clostridiales	Lachnospiraceae	*[Ruminococcus]*
4	*Bacteria*	Actinobacteria	Actinobacteria	Bifidobacteriales	Bifidobacteriaceae	*Bifidobacterium*
5	*Bacteria*	Firmicutes	Clostridia	Clostridiales	Ruminococcaceae	*Oscillospira*
6	*Bacteria*	Firmicutes	Clostridia	Clostridiales	Clostridiaceae	*SMB53*
7	*Bacteria*	Firmicutes	Clostridia	Clostridiales	Veillonellaceae	*Phascolarctobacterium*
8	*Bacteria*	Firmicutes	Clostridia	Clostridiales	Lachnospiraceae	*Dorea*
9	*Bacteria*	Firmicutes	Clostridia	Clostridiales	Clostridiaceae	*Clostridium*
10	*Bacteria*	Firmicutes	Erysipelotrichi	Erysipelotrichales	Erysipelotrichaceae	__
11	*Bacteria*	Firmicutes	Bacilli	Lactobacillales	Streptococcaceae	*Streptococcus*
12	*Bacteria*	Fusobacteria	Fusobacteriia	Fusobacteriales	Fusobacteriaceae	__
13	*Bacteria*	Firmicutes	Bacilli	Lactobacillales	Lactobacillaceae	*Lactobacillus*
14	*Bacteria*	Firmicutes	Bacilli	Lactobacillales	Leuconostocaceae	*Weissella*
15	*Bacteria*	Actinobacteria	Actinobacteria	Actinomycetales	Corynebacteriaceae	*Corynebacterium*
16	*Bacteria*	Proteobacteria	Gammaproteobacteria	Pseudomonadales	Moraxellaceae	*Enhydrobacter*

Note: The "_" in the table indicates unannotated species

Correlation between the metabolites of PNS and gut microbiota

Relative associations were observed using Spearman's correlations index shown in Fig. 6A. *Corynebacterium*, *Enhydrobacter* and *Phascolarctobacterium* were positively associated with the yield of GF_1, while *Blautia*, *Lactobacillus*, *Oscillospira*, *Roseburia*, *Streptococcus* and *Weissella* was inversely correlated with its contents. GRh_2 showed a positive association with the presence of *Blautia*, *Roseburia* and *Weissella*,

while *Oscillospira* and *Phascolarctobacterium* were inversely correlated with its concentration. Strong positive correlations such as *Bifidobacterium*, *Corynebacterium*, *Enhydrobacter*, *Lactobacillus*, *Roseburia*, *Streptococcus* and *Weissella* with the yield of PPD were also confirmed. PPT showed a greatly positive association with the presence of *Roseburia* and *Weissella*. Interestingly, compared with the metabolites of PPD-type ginsenosides, PPD-type ginsenosides showed a stronger association with those gut microbials (Fig. 6B). In general, gut microbials enriched in the LF-PF group were positively correlated with PNS biotransformation. Based on the analysis, the data provided a meaningful link to understand the PNS metabolic differences mediated by personalized gut microbiota.

Biotransformation of PNS by *B. adolescentis* and *L. rhamnosus*

To confirm metabolic capacity of specific bacteria species, *B. adolescentis* and *L. rhamnosus* were employed to evaluate the biotransformation of PNS. As the results, PNS were biotransformed to generate GF_1, GC-K, PPD and PPT, while the metabolic profiles of PNS mediated by *B. adolescentis* and *L. rhamnosus* were different (Fig. 7). In general, *B. adolescentis* has a stronger ability to metabolize PNS than *L. rhamnosus*, especially PPD-type saponins.

Discussion

In this paper, PNS could be metabolized by human gut microbiota. 16S rRNA gene sequencing technology was employed for analyzing the gut microbiota. Indeed, several metabolites have been reported as bioactive substances. GC-K is proved with potential anti-cancer effects through inducing cell apoptosis to inhibit tumor growth. Effects of GC-K on insulin resistance and abnormal vascular smooth muscle cell (VSMC) proliferation have also been evaluated[12, 13]. Some studies directly indicate that GC-K shows higher anti-proliferative effects on colon cancer than ginseng parent compounds, such as ginsenoside Rb_1 (GRb_1) [14]. Due to the increased hydrophobicity of GC-K, the absorption and distribution into tissue have also been improved to obtain higher plasma concentration than GRb_1[15]. Furthermore, GC-K is only generated by catalyzing microbial β-glycosidases which could not be secreted from mammalian cells[5]. The beneficial biotransformation mediated by gut microbiota in human intestine plays an inevitable role to achieve pharmaceutical activities of *P. notoginseng*, similar with other TCMs, such as Asian and American ginseng. It is reported that GRh_2 possesses antineoplastic effects to inhibit metastasis of HepG2 liver carcinoma cell[16]. GF_1 could prevent atherosclerosis by suppressing NF-κB signaling pathway and down-regulating inflammatory factors expression[17]. PPT and PPD, as the products of PPT-type and PPD-type saponins, have low toxicity, relative good stability and potent biological activities, such as ameliorating glucose tolerance and insulin resistance[18]. PPD also plays important roles in redox equilibrium and neuroprotection through modulating the level of ROS or influencing mitochondrial function[19].

The biotransformation of gut microbiota plays a crucial role to regulate the pharmaceutical activities of saponins[19]. We have collected stool samples from LF-PF and HF-HP diet volunteers. The different diet-pattern healthy subjects are good candidates for strategies aiming at investigating different gut microbiota profiles. Our results are congruent with those of previous studies with decreased Firmicutes/Bacteroidetes (F/B) ratio in human gut microbiota driven by high-fat dietary perturbations, while the lower-fat diet increased abundance of *Blautia* and *Faecalibacterium*[8]. In addition, the abundance of *Bifidobacterium* and *Roseburia* in the high-fiber diet group were relatively higher[20], but the abundance of *Oscillospira* increased in the high-protein diet group[21]. Intriguingly, reduced diversity has been reported in gut microbiota of western-diet-fed mice[22], while our data showed relatively higher alpha-diversity in HF-HP group than LF-PF group. The inconsistency indicated healthy human gut microbiota were more complex than mice under controlled fed condition. Analyzing the composition of individual gut microbiota in LF-PF group, the proportion of Firmicutes phyla were significantly predominant than other phyla. Furthermore, the visualized PCoA showed two clusters to discriminate the inter-group variation. The alpha-diversity differences between LF-PF and HF-HP groups indicated that alpha-diversity of gut bacterial communities could be reshaped by diet composition. Moreover, PNS could be hydrolyzed by β-glucosidases which is secreted by gut microbiota. Because β-glucosidase is differently secreted by specific gut microbial species, the yields of GRh_2, PPT and PPD showed significantly differences between the two groups. The results showed that GRh_2, PPT and PPD were more easily metabolized by gut microbiota of LF-PF group. In addition, the abundance of PPD-type secondary ginsenosides were higher than PPT-type secondary ginsenosides, which was the same with our previous study[7]. Interestingly, some specific gut microbials possess biotransformation preference pertinent to some stereochemical structures.

We explored the correlations between metabolic secondary ginsenosides and gut microbials. Interesting, *Roseburia* and *Weissella* were significantly and positively correlated with the yields of PPD, PPT and GRh_2, of which the relative contents in LF-PF group were significantly higher than those in HF-HP group. Furthermore, GRh_2 showed a positive association with the presence of *Blautia*. Strong positive correlations were analyzed between *Bifidobacterium* and the yield of PPD, while its content was also positively correlated with *Corynebacterium*, *Enhydrobacter* and *Lactobacillus*. *Bifidobacterium* is able to uptake oligosaccharides for the fermentative metabolism of hexoses and pentoses[23]. It has also been reported *B. adolescentis* is selective for 4-nitrophenyl-β-D-glucopyranoside (pNPG) to 4-nitrophenyl-β-D-xylopyranoside (pNPX), with very low activity against other β, 1→4 and β, 1→2 substrates[24]. Furthermore, *Weissella cibaria* also metabolizes pNPG[25]. Moreover, it was reported that most low G + C% Gram-positive Firmicutes, *Blautia*, *Lactobacillus*, *Roseburia* and *Streptococcus*, have stronger β-glucosidases activity than other species[26]. Altogether, *Bifidobacterium*, *Blautia*, *Lactobacillus*, *Roseburia*, *Streptococcus* and *Weissella* enriched in LF-PF group may interpret the metabolic difference of GRh_2, PPT and PPD between the two groups. Interestingly, we found that the correlation between GC-K and PPD with the above-mentioned bacteria had an opposite trend, probably because GC-K could be further metabolized to be PPD. Furthermore, *Bifidobacterium, Roseburia*

and *Weissella* showed strong and weak positive correlation with the PPD-type and PPT-type secondary ginsenosides, respectively. The abundance of *Bifidobacterium, Roseburia* and *Weissella* could be potential biomarkers to predict the metabolites of Dammarane saponins. However, the accurate bacterial function should be analyzed by metagenomic sequencing data in the future. Furthermore, due to an enterohepatic circulation of xenobiotics, it is also important to investigate PNS metabolic profile *in vivo* by systemically considering the gut microbiota and liver metabolism.

Consequently, the aim of this study was to investigate the correlation between metabolic differences and gut microbiota of two diet patterns. Because of individual variations among each group, analysis should focus on the inter-group differences rather than consistency within the same group. Therefore, our study focused on the beta-diversity of gut microbiota between HF-HP and LF-PF groups including six representative subjects in each group, which led to the metabolic differences of PNS. Moreover, both of quality and quantity differences of PNS metabolites were also observed in two groups, which indicated gut microbiota diversity led to the metabolic differences of PNS. Depending on gut microbiota composition or function analysis, we could anticipate drug and drug-metabolite exposure for personalized adjustment to the dosage of medicine. It may be better to consider patients' dietary habits with oral administration of PNS. However, detailed metagenomics and enlarged sample size should not be ignored to validate the relationship between specific bacteria species and the yields of PNS metabolites.

Conclusions

In this study, a LC-MS/MS method was used to relatively quantify five main PNS-metabolites, including ginsenoside F_1 (GF_1), ginsenoside Rh_2 (GRh_2), ginsenoside compound K (GC-K), protopanaxatriol (PPT) and protopanaxadiol (PPD), between HF-HP and LF-PF groups. The yields of GRh_2, PPT and PPD mediated by gut microbiota derived from LF-PF groups were much higher than HF-HP groups. The profiles of gut microbiota between the two group were significantly different through 16S rRNA sequencing. The genus *Blautia*, *Bifidobacterium*, *Roseburia*, *Ruminococcus* and *SMB53* ,enriched in LF-PF group, were positively correlated with PNS-metabolites . At the same time, strain experiments also confirmed that PNS can be metabolized by *B. adolescentis* and *L. rhamnosus* into the above-mentioned main products.

Abbreviations

16S rRNA, 16S ribosomal RNA; **DH-PPT**, didehydro-protopanaxatriol**; DMSO**, dimethyl sulphoxide; **F/B ratio**, the Firmicutes/Bacteroidetes (F/B) ratio; **GAM**, General anaerobic medium; **GC-K**, ginsenoside compound K; **GF_1**, ginsenoside F_1; **GRb_1**, ginsenoside Rb_1; **GRh_2**, ginsenoside Rh_2; **HF-HP diet**, high-fat and high-protein diet; **HPLC-ESI-MS/MS**, a high performance liquid chromatography-electrospray ionization tandem mass spectrometry; **LDA**, linear discriminative analysis; **LEfSe**, the linear discriminative analysis effect size; **LF-PF diet**, low-fat and plant fiber-rich diet; **OTUs**, operational taxonomic units; **PCoA**, principal component analysis; **PC**, principal component; **PCR**, Polymerase Chain Reaction; **PNS**, *Panax notoginseng* saponins; **PPD**, protopanaxadiol; **PPT**, protopanaxatriol; **QIIME**, Quantitative Insights Into Microbial Ecology; **TCMs**, traditional Chinese medicines; **VSMC**, vascular smooth muscle cell.

Declarations

Ethics approval and consent to participate

These procedures used for feces samples collection were approved by Ethics Committee of Central South University.

Consent for publication

All participates signed informed consent.

Availability of data and materials

The original data generated from this study are accompanied with the article as supplementary files.

Competing interests

The authors declare that they have no competing interests.

Funding

This research was supported by the National Natural Scientific Foundation of China (82074000, 81903784), the Hunan Provincial Natural Science Foundation of China (2020JJ4878), the Scientific Research Project of Department of Education of Hunan Province (20K136), and NHC Key Laboratory of Birth Defect for Research and Prevention (Hunan Provincial Maternal and Child Health Care Hospital, No. KF2020002).

Authors' contributions

WH H designed the experiments; L W and MY C participated in the experiments and analyzed the 16S rRNA sequencing data; L S, W Z and XP L provided the technical support and advices for the study; L W, XP L and WH H wrote the manuscript. All authors approved the final version of

manuscript.

Acknowledgements

We thank Mr. Yi-Cheng Wang in our institute for his technical support on mass spectrometry.

References

1. Gao S, Basu S, Yang Z, Deb A. M. H. Bioavailability challenges associated with development of saponins as therapeutic and chemopreventive agents. Curr Drug Target. 2012;13(14):1885–99.
2. Zhu D, Zhou Q, Li H, Li S, Dong Z, Li D, et al. Pharmacokinetic Characteristics of Steamed Notoginseng by an Efficient LC – MS/MS Method for Simultaneously Quantifying Twenty-three Triterpenoids. J Agric Food Chem. 2018;66(30):8187–98.
3. Kim DH. Gut microbiota-mediated pharmacokinetics of ginseng saponins. J Ginseng Res. 2018;42(3):255–63.
4. Xiao J, Chen H, Kang D, Shao Y, Shen B, Li X, et al. Qualitatively and quantitatively investigating the regulation of intestinal microbiota on the metabolism of panax notoginseng saponins. J Ethnopharmacol. 2016;194(2016):324–36.
5. Niu T, Smith DL, Yang Z, Gao S, Yin T, Jiang ZH, et al. Bioactivity and bioavailability of ginsenosides are dependent on the glycosidase activities of the A/J mouse intestinal microbiome defined by pyrosequencing. Pharm Res. 2013;30(3):836–46.
6. Xing R, Zhou L, Xie L, Hao K, Rao T, Wang Q, et al. Development of a systematic approach to rapid classification and identification of notoginsenosides and metabolites in rat feces based on liquid chromatography coupled triple time-of-flight mass spectrometry. Anal Chim Acta. 2015;867(2015):56–66.
7. Chen MY, Shao L, Zhang W, Wang CZ, Zhou HH, Huang WH, et al. Metabolic analysis of Panax notoginseng saponins with gut microbiota-mediated biotransformation by HPLC-DAD-Q-TOF-MS/MS. J Pharm Biomed Anal. 2018;150(2018):199–207.
8. Wan Y, Wang F, Yuan J, Li J, Jiang D, Zhang J, et al. Effects of dietary fat on gut microbiota and faecal metabolites, and their relationship with cardiometabolic risk factors: a 6-month randomised controlled-feeding trial. Gut. 2019;68(8):1417–29.
9. Dave M, Higgins PD, Middha S, Rioux KP. The human gut microbiome: current knowledge, challenges, and future directions. Transl Res. 2012;160(4):246–57.
10. Liu R, Hong J, Xu X, Feng Q, Zhang D, Gu Y, et al. Gut microbiome and serum metabolome alterations in obesity and after weight-loss intervention. Nat Med. 2017;23(7):859–68.
11. Guo Y-P, Chen M-Y, Shao L, Zhang W, Rao T, Zhou H-H, et al. Quantification of Panax notoginseng saponins metabolites in rat plasma with in vivo gut microbiota-mediated biotransformation by HPLC-MS/MS. Chin J of Nat Medicines. 2019;17(3):231–40.
12. Chen Y, Xu Y, Zhu Y. X. L. Anti-cancer effects of ginsenoside compound k on pediatric acute myeloid leukemia cells. Cancer Cell Int. 2013;13(1):24.
13. Chen L, Zhou L, Wang Y, Yang G, Huang J, Tan Z, et al. Food and Sex-Related Impacts on the Pharmacokinetics of a Single-Dose of Ginsenoside Compound K in Healthy Subjects. Front Pharmacol. 2017;8:636.
14. Wang CZ, Du GJ, Zhang Z, Wen XD, Calway T, Zhen Z, et al. Ginsenoside compound K, not Rb1, possesses potential chemopreventive activities in human colorectal cancer. Int J Oncol. 2012;40(6):1970–76.
15. Kim HK. Pharmacokinetics of ginsenoside Rb1 and its metabolite compound K after oral administration of Korean Red Ginseng extract. J Ginseng Res. 2013;37(4):451–56.
16. Shi Q, Shi X, Zuo G, Xiong W, Li H, Guo P, et al. Anticancer effect of 20(S)-ginsenoside Rh2 on HepG2 liver carcinoma cells: Activating GSK-3beta and degrading beta-catenin. Oncol Rep. 2016;36(4):2059–70.
17. Qin M, Luo Y, Lu S, Sun J, Yang K, Sun G, et al. Ginsenoside F1 Ameliorates Endothelial Cell Inflammatory Injury and Prevents Atherosclerosis in Mice through A20-Mediated Suppression of NF-kB Signaling. Front Pharmacol. 2017;8:953.
18. Deng J, Liu Y, Duan Z, Zhu C, Hui J, Mi Y, et al. Protopanaxadiol and Protopanaxatriol-Type Saponins Ameliorate Glucose and Lipid Metabolism in Type 2 Diabetes Mellitus in High-Fat Diet/Streptozocin-Induced Mice. Front Pharmacol. 2017;8:506.
19. Wang M, Li H, Liu W, Cao H, Hu X, Gao X, et al. Dammarane-type leads panaxadiol and protopanaxadiol for drug discovery: Biological activity and structural modification. Eur J Med Chem. 2020;189(2020):112087.
20. Leong C, Haszard JJ, Heath AM, Tannock GW, Lawley B, Cameron SL, et al. Using compositional principal component analysis to describe children's gut microbiota in relation to diet and body composition. Am J Clin Nutr. 2020;111(1):70–8.
21. Liu JP, Zou WL, Chen SJ, Wei HY, Yin YN, Zou YY, et al. Effects of different diets on intestinal microbiota and nonalcoholic fatty liver disease development. World J Gastroenterol. 2016;22(32):7353–64.
22. Turnbaugh PJ, Backhed F, Fulton L, Gordon JI. Diet-induced obesity is linked to marked but reversible alterations in the mouse distal gut microbiome. Cell Host Microbe. 2008;3(4):213–23.
23. Louis P, Hold GL, Flint HJ. The gut microbiota, bacterial metabolites and colorectal cancer. Nat Rev Microbiol. 2014;12(10):661–72.

24. Florindo RN, Souza VP, Manzine LR, Camilo CM, Marana SR, Polikarpov I, et al. Structural and biochemical characterization of a GH3 beta-glucosidase from the probiotic bacteria Bifidobacterium adolescentis. Biochimie. 2018;148(2018):107–15.
25. Lee KW, Han NS, Kim JH. Purification and characterization of beta-glucosidase from Weissella cibaria 37. J Microbiol Biotechnol. 2012;22(12):1705–13.
26. Dabek M, McCrae SI, Stevens VJ, Duncan SH, Louis P. Distribution of beta-glucosidase and beta-glucuronidase activity and of beta-glucuronidase gene gus in human colonic bacteria. FEMS Microbiol Ecol. 2008;66(3):487–95.

Figures

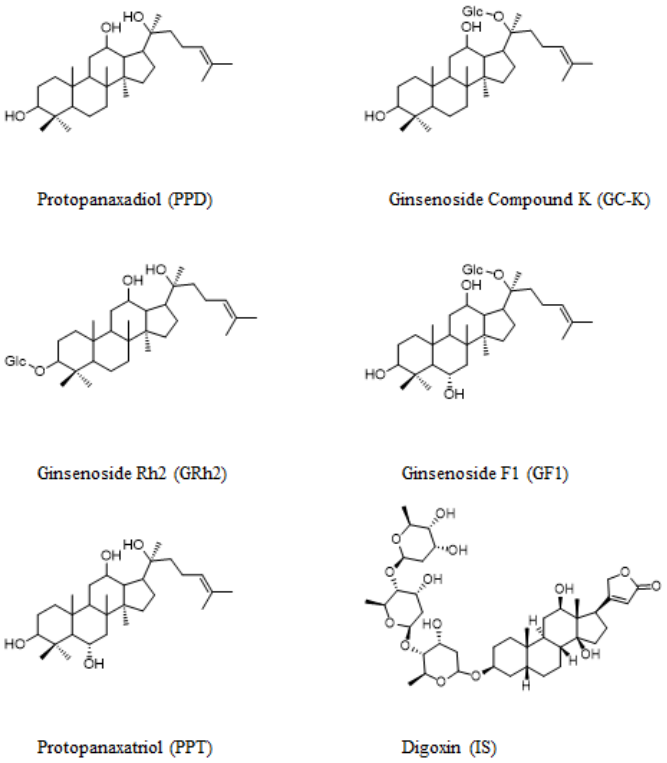

Figure 1

Chemical structures of P. notoginseng saponins metabolites

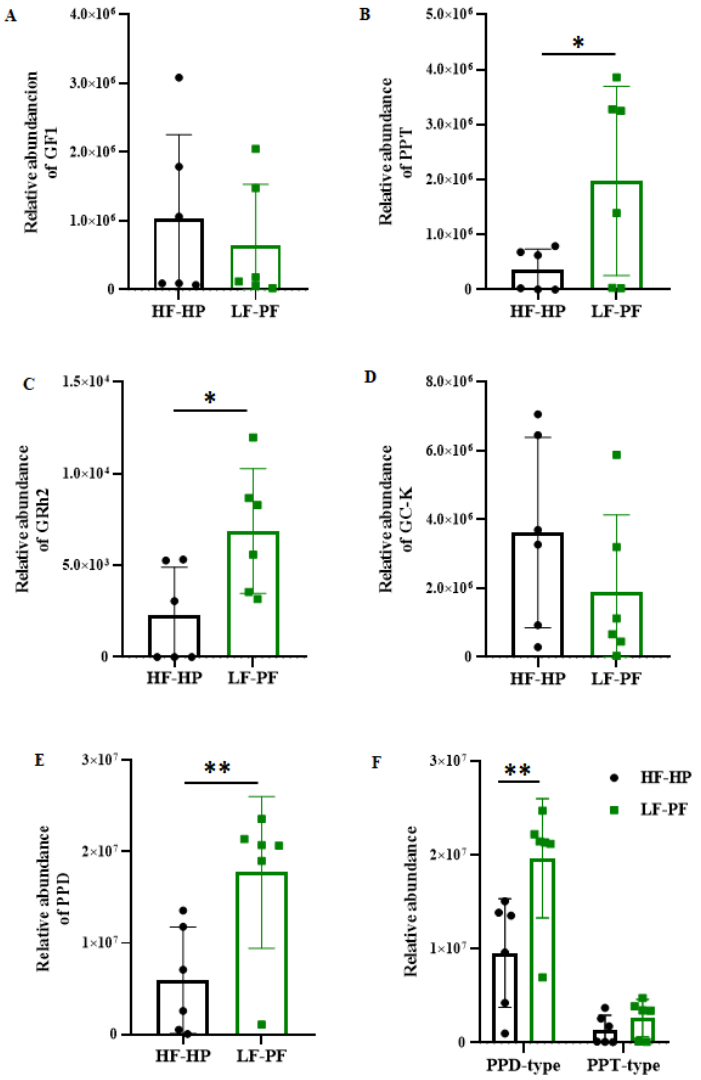

Figure 2

Chromatographic analysis of five main P. notoginseng saponins metabolites. The relative quantification of GF1(A), PPT(B), GRh2(C), GC-K(D) and PPD(E) in LF-PF and HF-HP diet groups; The relative quantification of PPT-type secondary ginsenosides and PPD-type secondary ginsenosides in LF-PF and HF-HP diet groups (F).

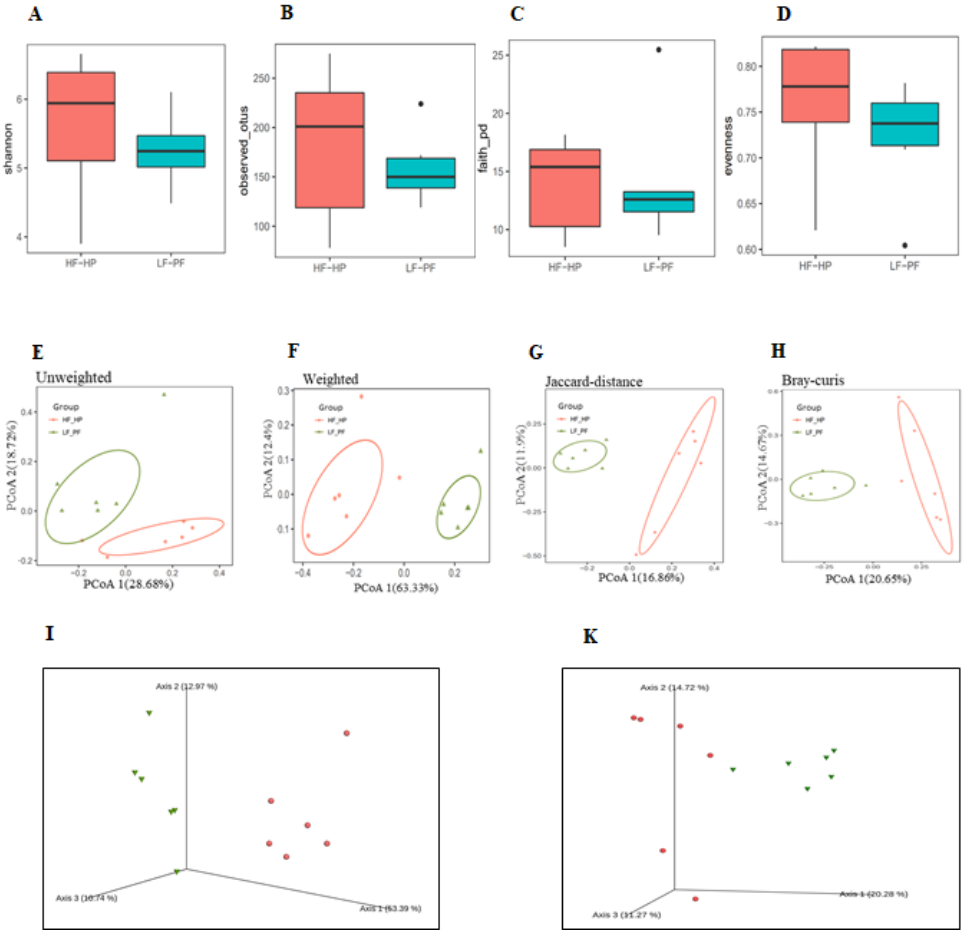

Figure 3

The alpha- and beta-diversity of the gut microbiota collected from LF-PF and HF-HP diet groups. Alpha-diversity analysis based on Shannon index (A), Observed OTUs(B), Faith's index(C) and Evenness index (D). Beta-diversity analysis based on Unweighted unifrac distance (E), Weighted unifrac distance (F and I), Jaccard distance(G) and Bray-Curtis distance (H and K). Each point represented a sample with colors different states. Red curve was composed of HF-HF diet adults and green curve was composed of LF-PF diet adults.

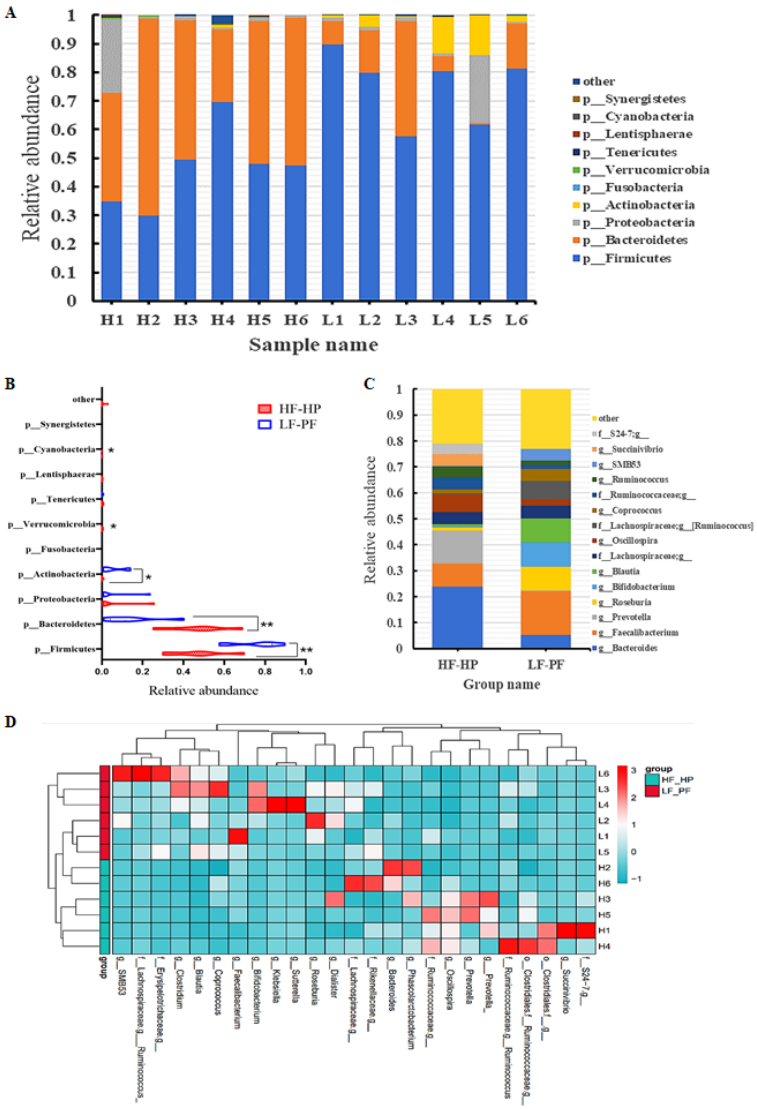

Figure 4

Microbial signatures of the gut microbiota in different diet groups. Phyla-level microbial classification of individual stool samples (A) and the two diet groups (B); Genus-level microbial classification of the two diet groups (C); A clustering analysis based on the abundance of the top 25 features (D).

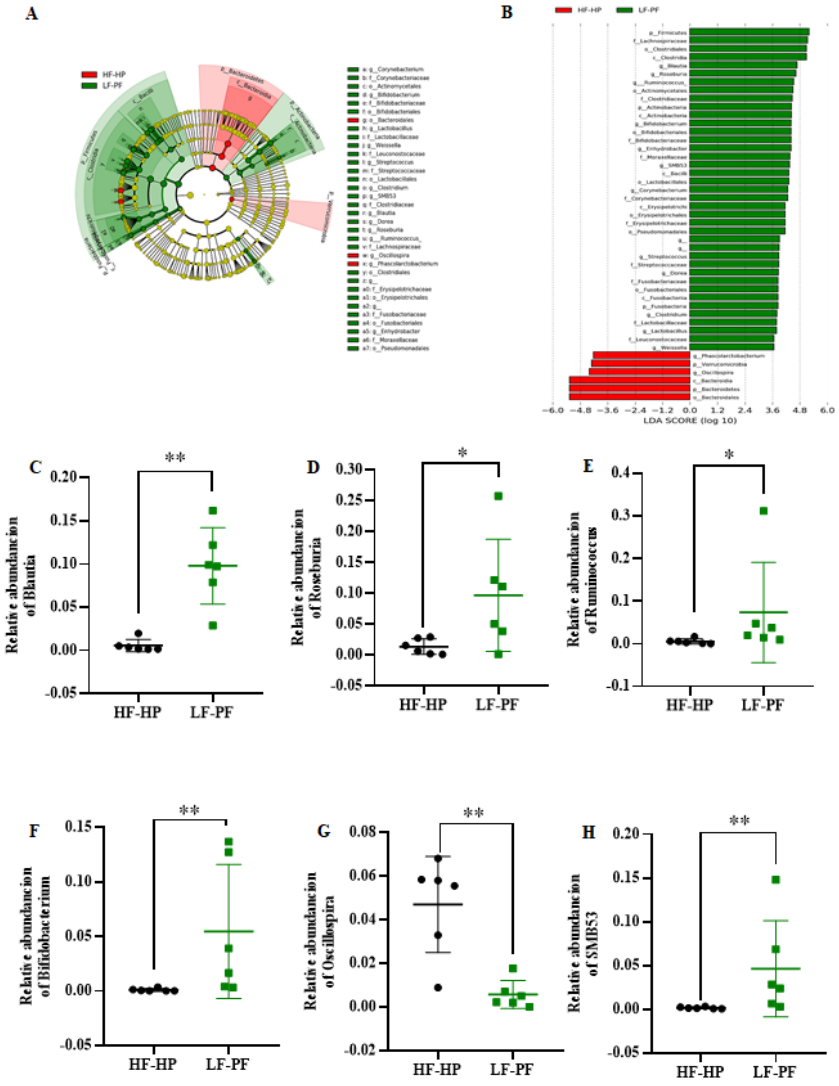

Figure 5

Taxonomic differences of gut microbiota between LF-PF and HF-HP diet groups derived from the LefSe method. Taxonomic cladogram with LEfSe for data analysis and visualization. Taxa with enriched levels in HF-HP and LF-PF groups (A); LDA scores (> 2) observed for individual taxa (B). Relative abundance of Blautia, Roseburia, Ruminococcus, Bifidobacterium, SMB53 and Oscillospira between the two group (C-H).

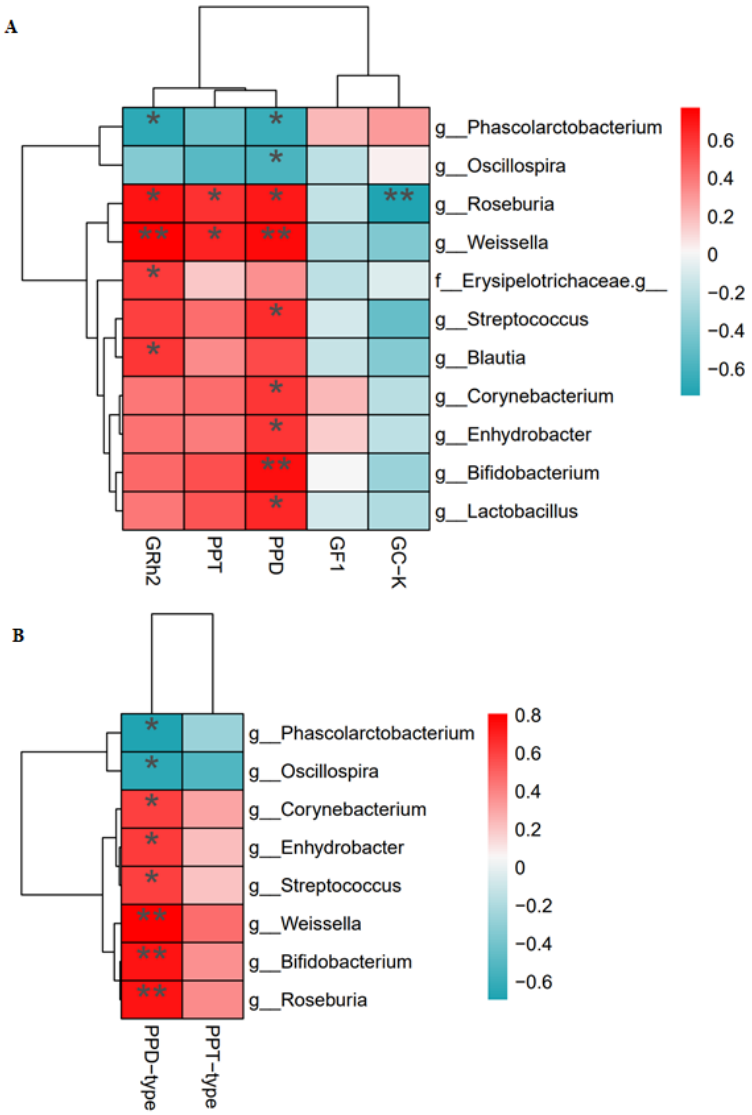

Figure 6

Heat map on Spearman's correlations among main metabolites and Taxonomic differences of gut microbiota between LF-PF and HF-HP diet groups.

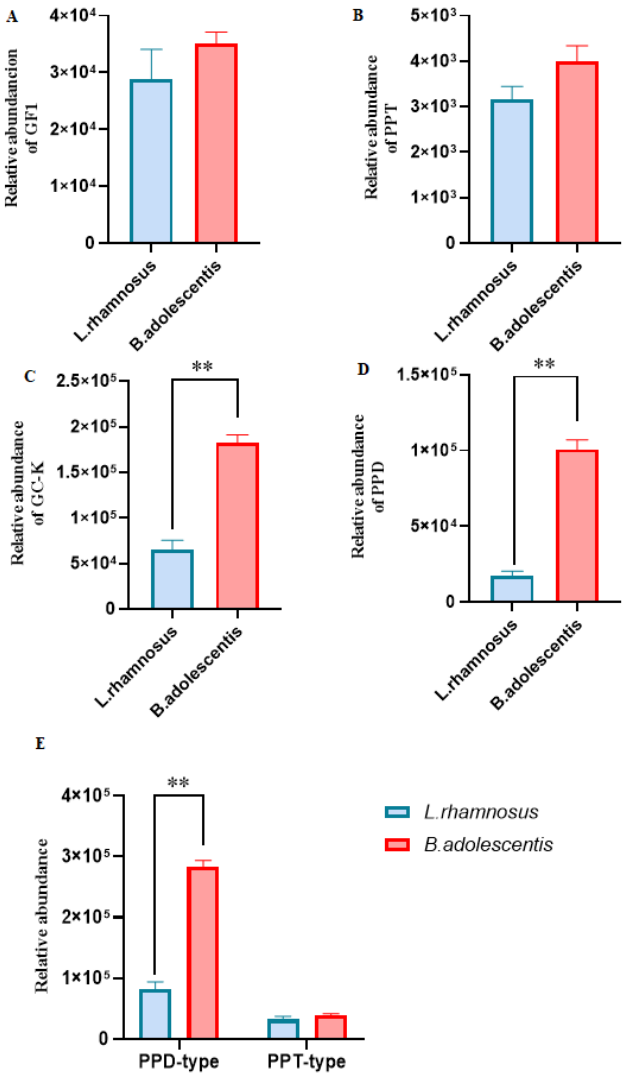

Figure 7

Chromatographic analysis of main P. notoginseng saponins metabolites bioconverted by selected microbials. The relative quantification of GF1(A), PPT(B), GC-K(C) and PPD(D) in B. adolescentis and L. rhamnosus; The relative quantification of PPT-type secondary ginsenosides and PPD-type secondary ginsenosides B. adolescentis and L. rhamnosus (E).

Supplementary Files

This is a list of supplementary files associated with this preprint. Click to download.

- CMHWH05062021GraphicAbstract.pptx
- CMHWH05062021SupplementaryFigures.pptx
- CMHWH05062021SupplementaryTables.docx